Toxicologic Pathology, 33:272–282, 2005

ISSN: 0192-6233 print / 1533-1601 online
DOI: 10.1080/019262390908362

2-Butoxyethanol Female-Rat Model of Hemolysis and Disseminated Thrombosis: X-Ray Characterization of Osteonecrosis and Growth-Plate Suppression

Danielle N. Lewis,[1,5] Abraham Nyska,[1,5] Kennita Johnson,[1] David E. Malarkey,[1] Sandy Ward,[1] Michael Streicker,[3] Shay Shabat,[4] Shyamal Peddada,[2] and Meir Nyska[4]

[1]*Laboratory of Experimental Pathology,* [2]*Biostatistics Branch, National Institute of Environmental Health Sciences, Research Triangle Park, North Carolina, USA*
[3]*Integrated Laboratory Systems (ILS), Research Triangle Park, North Carolina, USA, and*
[4]*Department of Orthopaedic Surgery, Sapir Medical Center, Kfar-Saba, Israel*
[5]*Co-Senior authors*

Abstract

We recently proposed a chemically induced rat model for human hemolytic disorders associated with thrombosis. The objective of the present investigation was to apply a noninvasive, high-magnification X-ray analysis, the Faxitron radiography system, to characterize the protracted bone damage associated with this 2-butoxyethanol model and to validate it by histopathology. Groups of female Fischer 344 rats were given 0, 250, or 300 mg of 2-butoxyethanol/kg body weight daily for 4 consecutive days. Groups were then sacrificed 2 hours or 26 days after the final treatment. The treated animals displayed a darkened purple-red discoloration on the distal tail. Histopathological evaluation, including phosphotungstic acid-hematoxylin staining of animals sacrificed 2 hours after the final treatment, revealed disseminated thrombosis and infarction in multiple organs, including bones. The Faxitron MX-20 specimen radiography system was used to image selected bones of rats sacrificed 26 days posttreatment. Premature thinning of the growth plate occurred in the calcaneus, lumbar and coccygeal vertebrae, femur, and ilium of the treated animals. Areas of decreased radiographic densities were seen in the diaphysis of the femur of all treated animals. The bones were then examined histologically and showed a range of changes, including loss or damage to growth plates and necrosis of cortical bone. No thrombi were seen in the animals sacrificed at 30 days, but bone and growth plate changes consistent with prior ischemia were noted. The Faxitron proved to be an excellent noninvasive tool that can be used in future studies with this animal model to examine treatment modalities for the chronic effects of human thrombotic disorders.

Keywords. 2-Butoxyethanol; hemolysis; thrombosis; osteonecrosis; growth plate; ischemia.

2-Butoxyethanol (BE) is a major environmental chemical utilized in the manufacturing of a wide range of domestic and industrial products, including surface coatings and household cleaning agents (Nyska et al., 1999b). It has been shown to cause acute hemolytic anemia in Fischer 344 rats upon metabolic activation to 2-butoxyacetic acid (BAA), with the hemolysis occurring more rapidly and severely in female rats (Ghanayem et al., 2000; Ezov et al., 2002). After 3 to 4 days of exposure to the chemical, thrombosis becomes apparent in several organs in the female rats, including the cardiac atrium, lungs, brain, submucosa of the anterior nasal septum, pulp of the incisor teeth, liver, coccygeal vertebrae, and femur (Nyska et al., 1999a, 1999b; Long et al., 2000; Ezov et al., 2002; Redlich et al., 2004). In addition, acute infarction occurs in the coccygeal vertebrae of the affected females, including that of the growth plate, and necrosis is seen grossly in the distal third of the tail (Nyska et al., 1999b; Shabat et al., 2004).

This acute and disseminated thrombosis and infarction in female rats induced by BE may result from vaso-occlusion, possibly triggered by acute hemolytic anemia with the potential release of procoagulant factors from destroyed erythrocytes, altered morphology and decreased deformability of erythrocytes, and a tendency of the red blood cells to aggregate and/or adhere to the endothelium (Ghanayem et al., 2000; Koshkaryev et al., 2003; Nyska et al., 2003).

The lack of bone or vascular lesions in male rats may be due to a more efficient elimination of BAA or decreased activity of aldehyde dehydrogenase, the enzyme responsible for the conversion of BE to its active metabolite (Aasmoe et al., 1998; Dill et al., 1998). In addition, less mature red blood cells have been shown to be more resistant to the effects of BE (Ghanayem et al., 2000; Koshkaryev et al., 2003).

Human erythrocytes are much less sensitive to the effects of BE than those of rats, requiring 100 times the concentration of BAA to develop fragility (Udden, 2002). The target organs for thrombosis and infarction found in this model, however, are similar to those observed in human disorders characterized by hemolysis and thrombosis, such as thalassemia and sickle cell disease (Smith, 1996; Eldor and Rachmilewitz, 2002; Ezov et al., 2002; Shabat et al., 2004). Furthermore, enhanced red blood cell and endothelial cell interaction has been demonstrated both in this animal model and human thrombotic diseases (Hovav et al., 1999; Yedgar et al., 1999; Koshkaryev et al., 2003). Currently, no effective

Address correspondence to: Dr. Abraham Nyska, Laboratory of Experimental Pathology, MD B3-06, National Institute of Environmental Health Sciences, 111 T. W. Alexander Drive, Research Triangle Park, North Carolina 27709-9998, USA; e-mail: nyska@niehs.nih.gov.

Abbreviations: BAA, 2-butoxyacetic acid; BE, 2-butoxyethanol; H&E, hematoxylin and eosin; Hct, hematocrit; Hgb, hemoglobin; MCH, mean cell hemoglobin; MCHC, mean cell hemoglobin concentration; MCV, mean cell volume; MRI, magnetic resonance imaging; NBF, neutral buffered formalin; PCV, packed cell volume; PTAH, phosphotungstic acid-hematoxylin; RBC, red blood cells; WBC, white blood cells.

or easy treatment exists for these conditions in man (Smith, 1996; Reed and Vichinsky, 1998; Eldor and Rachmilewitz, 2002). Previous animal models for these diseases have been either invasive or ineffective (Norman et al., 1998). This rat model of disseminated thrombosis induced by BE is a novel and noninvasive tool mimicking human hemolytic disorders associated with thrombosis.

Magnetic resonance imaging (MRI) has been used recently to study BE-induced bone injury in these rats. The MRI examination, however, neither identified a specific lesion nor distinguished the growth plate and diaphysis of the vertebrae (Shabat et al., 2004). That normal radiographs are not adequate for the diagnosis of aseptic osteonecrosis in human thrombotic diseases, such as sickle cell disease (Smith, 1996), has been demonstrated. The need exists, therefore, for a high-resolution imaging technique to aid in the diagnosis of this disease manifestation. Our goal was to determine whether a noninvasive, high-magnification X-ray imaging system, Faxitron MX-20 Digital, could reveal the bone lesions related to ischemia and thrombosis in the BE rat model. We hypothesized that the Faxitron could be applied to this animal model, providing high-quality images that could be used in additional applications testing various treatment modalities for the prevention of chronic complications of hemolytic disorders associated with thrombosis, such as bone infarction that occurs in thalassemia and sickle cell disease.

Female Fischer 344 rats were treated with either 250 or 300 mg/kg body weight of BE for 4 consecutive days. The dose of 250 mg/kg was shown in previous experiments (Ezov et al., 2002) to be the most appropriate dose to produce disseminated thrombosis. A dosage of 300 mg/kg was utilized to determine whether more widespread and severe alterations would develop in the skeleton secondarily to an increased incidence of thrombosis. Ghanayem et al. (1990) performed acute exposure toxicokinetic studies with BE administered as an IV bolus to 3–4-month-old male Fischer rats at doses of 31.35, 62.5, and 125.0 mg/kg; (dose volume = 1 ml/kg). Results indicated the Cmax, AUC and Cl_8 of BE and BAA (the proximate metabolite of BE). Cmax and AUC were increased, whereas Cl_8 decreased as the BE dose increased. These results suggested that the administration of 300 mg/kg would result in a higher Cmax and AUC than would 250 mg/kg.

The bones were examined histologically immediately after the final dose and by radiography and subsequent histology 26 days later. Our findings indicate a strong correlation between histological alterations and X-ray images, suggesting that the Faxitron imaging system possesses the sensitivity and specificity to detect bone lesions in this chemically induced model of disseminated thrombosis and bone necrosis in rats.

Materials and Methods

Chemicals, Animals, Treatments, and Experimental Procedures

2-Butoxyethanol of >99% purity was purchased from Sigma-Aldrich Chemical Co. (Rehovot, Israel). Female F344 rats 11 weeks of age were obtained from Taconic Farms (Germantown, NY) and provided the NTP 2000 diet (Zeigler Brothers, Gardners, PA) and water ad libitum. The animals were singly housed and allowed a period of acclimation to the facility conditions (18–26°C, 30–70% relative humidity, 12-hour light/dark cycle) before beginning the study. All procedures, care, and treatment of the rats were in accordance with the principles for humane treatment outlined by the Guide for the Care and Use of Laboratory Animals of the National Institutes of Health (Institute of Laboratory Animal Resources, 1996). The study was conducted following the review and approval of the Committee for Ethical Conduct in the Care and Use of Laboratory Animals at Integrated Laboratory Systems (ILS, Research Triangle Park, North Carolina 27709, USA) and after being found in compliance with the rules and regulations set forth. Control animals used in the X-ray analyses were derived from a previous BE study. The animal husbandry in the study was the same except for the age of the rats, which were 6–7 weeks old at the initiation of the experiment.

Dosing solutions of BE were prepared daily immediately prior to each dosing by mixing with tap water to obtain a dose volume of 5 ml/kg body weight and administered to the rats by gavage. Oral administration of BE is known to induce thrombosis in rats and is therefore the best available method of dosing. At study commencement, test groups were administered either 250 or 300 mg BE/5 ml tap water/kg body weight (Table 1). Control groups were administered tap water only. Animals were randomly assigned to treatment groups using a by-body-weight stratification procedure. Test groups received 4 consecutive daily treatments; the first day of dosing was regarded as day 1. The animals were observed approximately 24 hours after each dose and body weights were measured just prior to the first dosing and at termination.

Animals were sacrificed by CO_2 asphyxiation. Animals from groups 1, 2, and 3 were sacrificed and necropsied approximately 2 hours after the fourth dose. Animals from groups 4, 5, and 6 were sacrificed and necropsied at 30 days (26 days after the final treatment). From each animal euthanized 2 hours after the fourth dose, blood was immediately collected from the retroorbital venous plexus and placed into EDTA tubes. The following hematological parameters were evaluated: red blood cell (RBC) and white blood cell (WBC) counts, hemoglobin concentration (Hgb), hematocrit (Hct), mean cell volume (MCV), mean cell hemoglobin (MCH), mean cell hemoglobin concentration (MCHC), platelet count, and packed cell volume (PCV). For the cell blood count, the

TABLE 1.—Experimental study design showing number of animals in each group at study termination.

Test group	Amount of BE received (mg/kg/day for 4 days)	Day of sacrifice	Number of animals examined: Hematology	Histopathology	Faxitron
1	0	4	5	5	0
2[a]	250	4	3	3	0
3[b]	300	4	3	7	0
4	0	30	0	3	3
5[c]	250	30	0	2	2
6[d]	300	30	0	1	1

[a] 2 animals died before day 4 (40% mortality rate) and were not included in the histopathological examination due to autolysis.
[b] 4 animals died before day 4 (80% mortality rate) but were still examined histologically; 2 animals were added to this group from group 6.
[c] 3 animals were saved for future experiments; 0% mortality in this group.
[d] 4 animals died before day 30 (80% mortality rate); 2 were examined histologically at 4 days and were placed in group 3.

samples were assayed using the Technicon H-1 hematology analyzer (Bayer Corporation, Tarrytown, NY).

To monitor RBC parameters, spun microhematocrit was determined for each specimen and compared with automated hematocrit, which was calculated from the directly measured RBC and MCV. Control products were assayed after every specimen. For WBC differential data, Wright-Giemsa-stained smears were prepared, and manual WBC differential counts were performed on at least the first sample in the control group, as well as any other samples with an abnormal count. Manual differentials were performed on all smears from treated animals. In cases in which the two counts did not agree, the manual value was reported. RBC and platelet morphology was also examined. The blood smears were stained using the Ames Hema-Tek II automated slide stainer (Bayer Corporation, Ames Division, Elkhart, IN) For reticulocyte counts, equal amounts of whole blood and New Methylene Blue stain were allowed to incubate at room temperature for at least 15 minutes. Blood smears were prepared and examined to determine the percent reticulocytes per 1,000 RBCs. The percent value was multiplied by the RBC count to determine the absolute number of reticulocytes per microliter of blood.

Necropsy and Handling of Tissue

Animals were sacrificed on days 4 and 30 (Table 1) by CO_2 asphyxiation, and a complete necropsy and macroscopic examination were performed on each animal. The skin was removed from the body, and the skeleton was kept intact. The complete carcass was fixed in a splayed position for 4–5 days in 10% neutral buffered formalin (NBF) and then transferred to 70% histology-grade ethyl alcohol.

Imaging Procedures

The Faxitron Specimen Radiography System Model MX-20 Digital (Faxitron X-ray Corporation, Wheeling, IL) was used to acquire high-magnification, X-ray images of the skeletons of 3 control animals and 3 treated animals (one from the 300 mg/kg/day dose group and 2 from the 250 mg/kg/day dose group) sacrificed on day 30. The Faxitron MX-20 model has a 20-μm nominal focal spot, a 57.2-cm fixed source-to-image distance, and a 5.08-cm $\times$ 5.08-cm field-of-view CCD camera. In each animal, the tail and head were disarticulated from the skeleton and radiographs were taken of the proximal coccygeal vertebrae (1 cm from tail base), distal coccygeal vertebrae (10 cm from tail base), left and right tarsus, the sixth lumbar vertebra, left and right head of the femurs, left and right diaphyses of the femurs, and left and right proximal tibiae. Images were acquired at 30 kV, 0.3 mA, and automatically timed at approximately 1.75 seconds. The image size was 1024 $\times$ 1024 pixels. Radiographs were taken at both low ($\times$1.5) and high ($\times$3) magnification for each bone. Magnification was achieved by adjusting the source-to-object distance: 38.1 cm for $\times$1.5 and 19.1 cm for $\times$3. All irregularities in bone structure seen in the radiographs were noted.

Subepiphyseal and epiphyseal bone densities for each bone were measured using ImageJ software (National Institutes of Health) based on the pixel intensity over an area of 30 $\times$ 20 pixels. Bone densities for the proximal tibia were measured over an area of 100 $\times$ 200 pixels. The ratio of the epiphyseal density to the subepiphyseal density was then calculated for each bone.

Trimming of Tissue from Animals Sacrificed on Day 4

The eyes, heart, lungs, liver, and carcass were collected in 10% NBF. The eyes, heart, lungs, liver, nasal cavity, coccygeal vertebrae, femur, and proximal tibia were histologically processed. The bones of animals from all sacrifice periods were prepared for histopathological evaluation. Soft tissues were evaluated only in those animals sacrified immediately following the last dose, in order to confirm the presence of antemortem disseminated thrombosis. Tissues were embedded in paraffin, sectioned at 5–6 μm, and stained with hematoxylin and eosin (H&E) for microscopic examination (Chhabra et al., 1990). All bony tissues were decalcified prior to histological processing using Decalcifier II from Surgipath (Surgipath Medical Industries Inc., Richmond, IL). The nasal cavity was sectioned at 3 levels (Boorman et al., 1990). From the coccygeal vertebrae, 3 1-cm, mid-sagittal longitudinal sections (proximal, middle, and distal) were prepared.

All of the prepared tissue sections were examined microscopically, and several were chosen for special staining. Phosphotungstic acid-hematoxylin (PTAH) stain was used to illustrate fibrin in the thrombi as previously demonstrated (Momotani et al., 1985; Halvorsen et al., 1994). Matching sections from control animals were also taken for staining.

Trimming of Tissue from Animals Sacrificed on Day 30

After X-ray imaging, the bones were decalcified using Rapid Decalcifier (Apex Engineering Products Corporation, Aurora, IL) for a period of at least 4 hours and trimmed for histological sectioning. The following sections were taken for histology: proximal coccygeal vertebrae (1 cm from tail base), distal coccygeal vertebrae (10 cm from tail base), right and left ilium, right and left proximal femur, right and left distal femur and proximal tibia, right and left tarsus, and the sixth lumbar vertebra. Tissues were embedded in paraffin, sectioned at 5–6 μm, and stained with H&E for microscopic examination (Chhabra et al., 1990).

Upon histological examination, photographs were taken, and the width of the growth plate was measured in the head of the femur, distal femur, proximal tibia, and lumbar vertebra using ImageJ software (National Institutes of Health) for a control and an animal treated with 250 mg/kg/day BE. A micrometer was used to calibrate the measurements.

Statistical Analysis

The Dunnett's test was used to make comparisons between each treatment group (250 mg/kg/day and 300 mg/kg/day) and the control group for the decrease in mean body weight between the beginning of the experiment and its termination on day 4. This test was also used to analyze the hematological data for the animals sacrificed on day 4. Only 2 hematological parameters—the RBC and the MCV—were analyzed due to small sample size and experience in previous studies with the same model indicating that these factors best reflect the hematotoxicity of BE. Due to apparent heterogeneity of the data, these parameters were analyzed after performing log transformation. Each of the treated groups was compared with the control group. The SAS statistical software package (Release 8.2) was used to analyze these variables.

The Mann–Whitney–Wilcoxon nonparametric test was used to analyze parameters from the radiographic measurements. Because of the small sample size, only 2 bones were selected for statistical analysis. Due to the consistency in the lesions seen in the X-ray images, the lumbar vertebrae and the calcaneus bones were chosen. The ratio of the epiphyseal density to the subepiphyseal density was analyzed for these bones, comparing treated animals to controls.

Results

Clinical Signs and Body Weights

All of the treated animals began to have red-stained bedding 1 day after the first dose was given; this coloration continued for 1 to 2 days. The treated animals all also began to have a darkened discoloration on the tip of the tail on day 3, which became worse over time (Figures 1a–1b); 2 of the treated animals had lost the tip by 3 weeks. None of the control animals experienced any abnormal clinical signs throughout the study period.

All test animals sacrificed following the final dose on day 4 experienced an 8–16% decrease in body weight at the scheduled necropsy date. A statistically significant decrease occurred in mean body weight from the initiation of the experiment and the termination on day 4 for each of the treated groups compared to the control group ($p < 0.05$). No dose-related decrease in mean body weight occurred between the 2 treatment groups. In addition, 2 out of the 5 animals from the 250 mg/kg/day dose group (group 2) and 4 out of the 5 animals from the 300 mg/kg/day dose group (group 3) died before their scheduled necropsy date on day 4 (Table 1). These animals experienced a 6.8–12.6% decrease in body weight between the beginning of the experiment and their death. The animals in group 3 that died early were included in the histological examination. The animals in group 2 that died early were not included due to autolysis and inability to examine the tissue histopathologically.

The treated animals sacrificed at day 30 experienced a loss in body weight during the treatment period but then recovered, experiencing an overall gain in weight during the course of the study. Four of the 5 animals from the 300 mg/kg/day dose group (Group 6) died before their scheduled necropsy date on day 30. Two of these animals died on day 4 and were included in the histological examination with the animals from Group 3 (Table 1).

Hematology for Animals Sacrificed on Day 4

In agreement with previous findings (Ezov et al., 2002), gavage administration of 250 or 300 mg 2-BE/kg for 4 days resulted in severe, acute, regenerative hemolytic anemia in all animals sacrificed on day 4.

Macroscopic Abnormalities

In agreement with previous findings (Ezov et al., 2002), the most common abnormalities among the BE-treated animals sacrificed on day 4 included dark kidneys and spleen, enlarged spleen, pale liver, distention of the urinary bladder with red fluid, and a dark discoloration on the tip of the tail. No significant differences were observed in the gross findings between the 250 mg/kg treated group and the 300 mg/kg treated group.

The only common finding among the treated animals sacrificed on day 30 was a darkened purple-red discoloration on the distal third of the tail, which was noted in all 3 treated animals sacrificed on that day.

Histopathological Findings for Animals Sacrificed on Day 4

In agreement with previous findings (Ezov et al., 2002), thromboses were seen in several organs in both the 250 mg/kg-treatment group and the 300 mg/kg-treatment group. No thrombi were observed in any of the control animals. Affected organs included the nasal cavity, incisor teeth, coccygeal vertebrae, femur, liver, and lungs. The vascular thrombi were occlusive and consisted of amorphous granular material. The occurrence of antemortem fibrin thrombi was confirmed using PTAH staining (Figures 2a–3b). The thrombi appeared both tangled (knot-like) and massed, as described previously (Momotani et al., 1985).

Bone changes were in agreement with previously described findings (Nyska et al., 1999b), and are summarized in Table 2. Growth plate alterations, such as those observed in the tail vertebra, consisted of degeneration of chondrocytes in the proliferative zone and early hypertrophied zone. Areas of degeneration exhibited a loss of chondrocytes, pallor of the cartilage matrix, and granularity and/or fragmentation with fibrillation. Chondrocytes located immediately adjacent to the degenerate areas were often disorganized, resulting in distortion of growth plate architecture.

Some of the osteocyte lacunae in the cortical and trabecular bone of both the femur and the coccygeal vertebrae showed apoptotic bodies or were empty. Most of the thrombi in the femur occurred near the stifle joint and were intramedullary, whereas most of the thrombi in the coccygeal vertebrae occurred in the periosteal and subcutaneous tissue. No positive identification of fibrin by PTAH staining was observed in any of the control animals.

X-Ray Image Analysis and Histopathological Findings for Animals Sacrificed on Day 30

Lesions were seen in several bones in all of the treated animals (Table 2). No differences were detectable in the lesions between the animals treated with 250 mg/kg/day of BE and those treated with 300 mg/kg/day. Because of this fact and the small sample size, the 3 treated animals were analyzed together, regardless of treatment group. The most common findings were a premature closure of the growth plate, alteration in the shape of the growth plate, and decreased radiographic density (e.g., increased radiolucency) in the medullary cavity and the subepiphyseal area (Figures 4a–4d, 6a–6d). The radiolucent areas in the shaft of the long bones includes the marrow area and extends to the cortex causing thinning of the cortex. This is demonstrated in the histological findings of these areas by dead osteocytes and necrotic bone lamella. A premature closure of the growth plate (e.g., growth plate is not evident) of both calcaneus bones occurred in all 3 treated animals. A loss of the triradiate cartilage of the acetabulum was apparent in all 3 treated animals. No lesions were seen in any of the control animals. A statistically significant increase in the ratio of the epiphyseal density to the subepiphyseal density occurred in the treated animals, compared

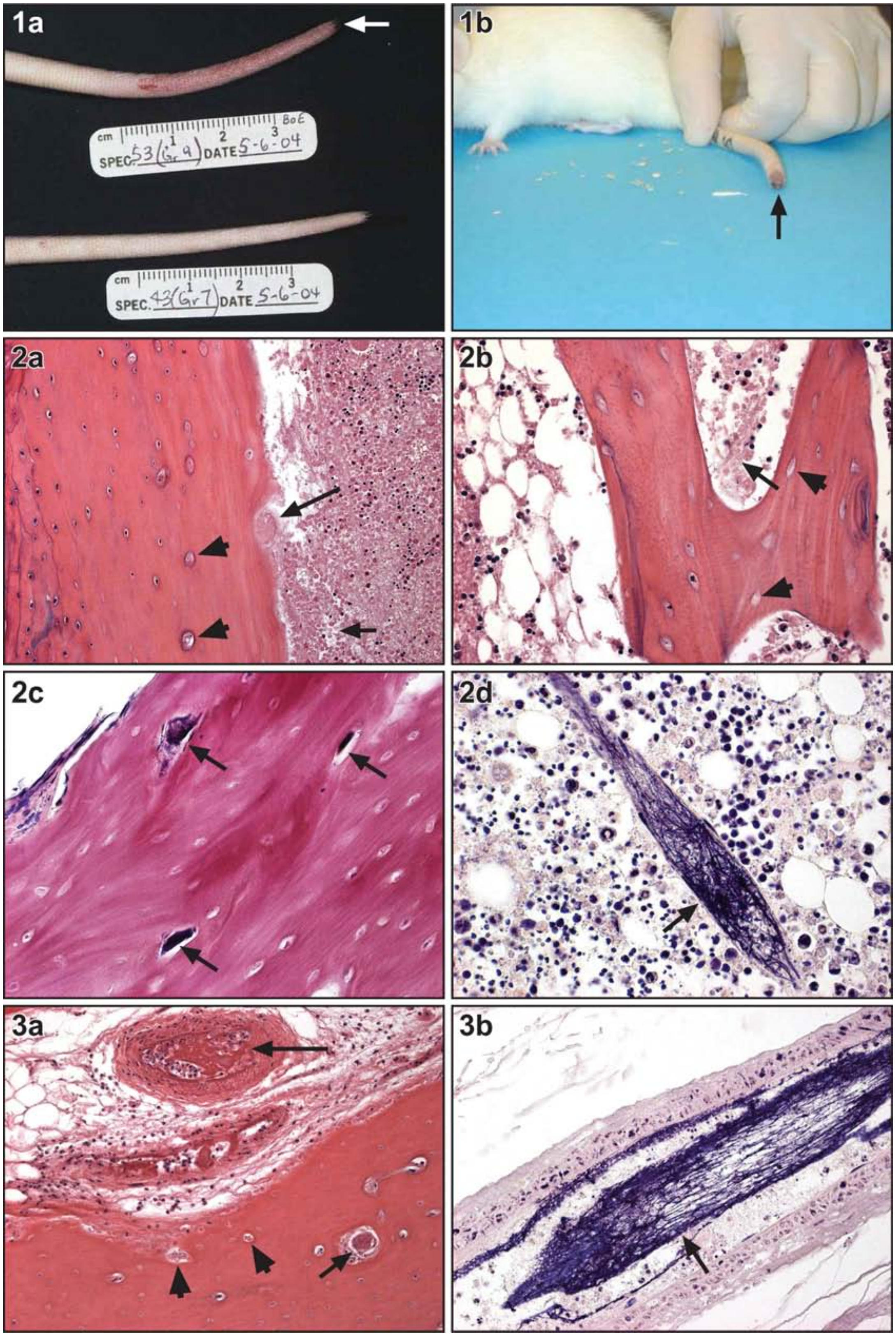

FIGURE 1.—Fischer 344 female rats. (a) Distal tail necrosis in rat treated with 250 mg/kg/day BE for 4 days (arrow) vs. normal tail of control. (b) Loss of the distal tail (arrow) 3 weeks after exposure to BE. 2.—Fischer 344 female rats. (a) Cortical bone thrombosis (long arrow), bone marrow necrosis (short arrow) and osteocytic necrosis (arrowheads) in femur; 300 mg/kg/day BE for 4 days. H&E. ×20. (b) Bone marrow necrosis (arrow) and trabecular bone necrosis (arrowheads) in femur; 300 mg/kg/day BE for 4 days. H&E. ×40. (c) Fibrin thrombi (arrows) in cortical bone of femur; 300 mg/kg/day BE for 4 days. PTAH. ×20. (d) Fibrin thrombus (arrow) in medullary cavity of femur; 300 mg/kg/day BE for 4 days. PTAH. ×60. 3.—Fischer 344 female rats. (a) Periosteal thrombosis (long arrow), cortical-bone thrombosis (short arrow) and osteocytic necrosis (arrowheads) in coccygeal vertebra; 250 mg/kg/day BE for 4 days. H&E. ×20. (b) Fibrin thrombus (arrow) in tail artery; 250 mg/kg/day BE for 4 days. PTAH. ×40.

TABLE 2.—Incidence of selected Faxitron-radiography findings for animals sacrificed on day 30; correlation with histopathological findings.

Faxitron findings	Group 4, control	Groups 5 and 6, treated	Confirmed by histopathology	Histopathological findings (%)
Proximal tail				
Closure of growth plate	0/3[a]	1/3	1/3	Growth-plate necrosis (33)
Distal tail				
Irregular shape of growth plate	0/3	3/3	3/3	Necrosis of growth-plate (100), cortical (100) and trabecular (66) bone, bone marrow (100), and skeletal muscle (66);
Lytic areas in subepiphysis	0/3	1/3	3/3	Granulomatous inflammation of bone marrow (66)
Lumbar vertebra				
Closure of growth plate	0/3	3/3	3/3	Thinning of growth plate[b] (100)
Ilium				
Loss of triradiate cartilage	0/3	3/3	3/3	Loss of triradiate cartilage[c] (66)
Femur				
Closure of growth plates	0/3	3/3	3/3	Necrosis of growth-plate (33), cortical bone (66);
Decreased density in medullary cavity	0/3	3/3	2/3	Thinning of growth plate [d,e] (100)
Tibia				
Closure of growth plate	0/3	1/3	3/3	Thinning of growth plate (100)
Tarsus				
Closure of growth plate of calcaneus	0/3	3/3	3/3	Loss of growth plate[f] (100)
Decreased density in medullary cavity of tarsal bones	0/3	2/3	0/3	

[a] No. of animals with finding/No. of animals examined.
[b] Width of growth plate 0.54 mm in treated animal vs. 0.75 mm in control.
[c] Area of interest not included in section for other treated animal.
[d] Width of growth plate in head of femur 0.68 mm in treated animal vs. 0.83 mm in control.
[e] Width of growth plate in distal femur 1.60 mm in treated animal vs. 1.79 mm in control.
[f] Width of growth plate 1.04 mm in treated animal vs. 1.60 mm in control.

to the control animals, for both the lumbar vertebrae ($p = 0.05$) and the calcaneus bones ($p = 0.01$). The ratios of the epiphyseal density to the subepiphyseal density are shown in Table 3.

Histological examination revealed lesions in treated animals in all of the bones examined (Table 2). No lesions were observed in the control animals. The bones most consistently affected histologically were the distal coccygeal vertebrae and the calcaneus bones (Figures 5a–5d, 7a–7d). The distal coccygeal vertebrae manifested the most severe damage, which corresponded to the clinical signs of the treated rats. Histopathology consisted of severe regional ischemia (usually the central region) of the growth plate, as described previously (Nyska et al., 1999b). These histological changes caused the radiolucency in the subepiphyseal area. Measurements showed a thinning in some growth plates of the treated animals, compared to controls, which was also noted during histological examination (Table 2). In vertebra where thinning of growth plate was noted (e.g., lumbar vertebra, tibia), all layers were present, without apparent loss of cells.

TABLE 3.—Mean and standard error of the epiphyseal to subepiphyseal density ratios for animals sacrificed on day 30.

Bone measured	Group 4 control	Groups 5 and 6 treated
Proximal tail	0.90 ± 0.05	0.90 ± 0.05
Distal tail	0.80 ± 0.04	0.91 ± 0.03
Lumbar vertebra	0.72 ± 0.09	0.91 ± 0.05[a]
Left proximal tibia	1.23 ± 0.06	1.18 ± 0.05
Right proximal tibia	1.34 ± 0.14	1.12 ± 0.03
Left calcaneus	0.95 ± 0.05	1.32 ± 0.12[b]
Right calcaneus	1.02 ± 0.02	1.64 ± 0.52[b]

[a] $p = 0.05$ vs. control (Mann–Whitney–Wilcoxon nonparametric test).
[b] $p = 0.01$ vs. control (Mann–Whitney–Wilcoxon nonparametric test).

DISCUSSION

In agreement with previous studies (Ezov et al., 2002), our research demonstrated that BE induces acute hemolytic anemia, disseminated thrombosis, and bone infarction in female F344 rats at doses of 250 mg/kg/day and 300 mg/kg/day administered for 4 days and premature closure and infarction of growth plates in 30 days, or 26 days after the final treatment.

Through special staining, we confirmed the presence of antemortem fibrin thrombi. Extensive bone necrosis was also found; empty osteocytic lacunae served as our diagnostic criterion (Nyska et al., 1999b; Zhao et al., 2000; Ezov et al., 2002; Shabat et al., 2004). We also demonstrated that the Faxitron Radiography System is effective in producing high-magnification images of bone lesions that can be correlated with histopathological changes. The Faxitron was not used in the animals sacrificed on day 4, because the changes in opacity due to bone pathology can only be detected after a few weeks when loss of bone, deposition of woven bone, and/or calcification occur (Imhof et al., 1997).

The cause of death was most likely attributable to the severe anemia, hypoxia, and/or thrombosis induced by BE. One of the objectives of this experiment was to test if an increased dose of 300 mg/kg would result in more widespread and severe alterations secondary to thrombosis, without increasing mortality. Because such a high number of the rats receiving this dose died early in the study, 300 mg/kg/day was proven to be above the maximum tolerated dose. In addition, because no noticeable differences in the severity of the lesions were noted between the dosages, the 250 mg/kg/day BE was demonstrated to be an appropriate dose for this model. Previous experiments have indicated that this dose is effective in producing thrombosis with only sporadic cases of mortality, most likely related to severe anemia and hypoxia (Ezov et al., 2002). These studies also illustrated the necessity of

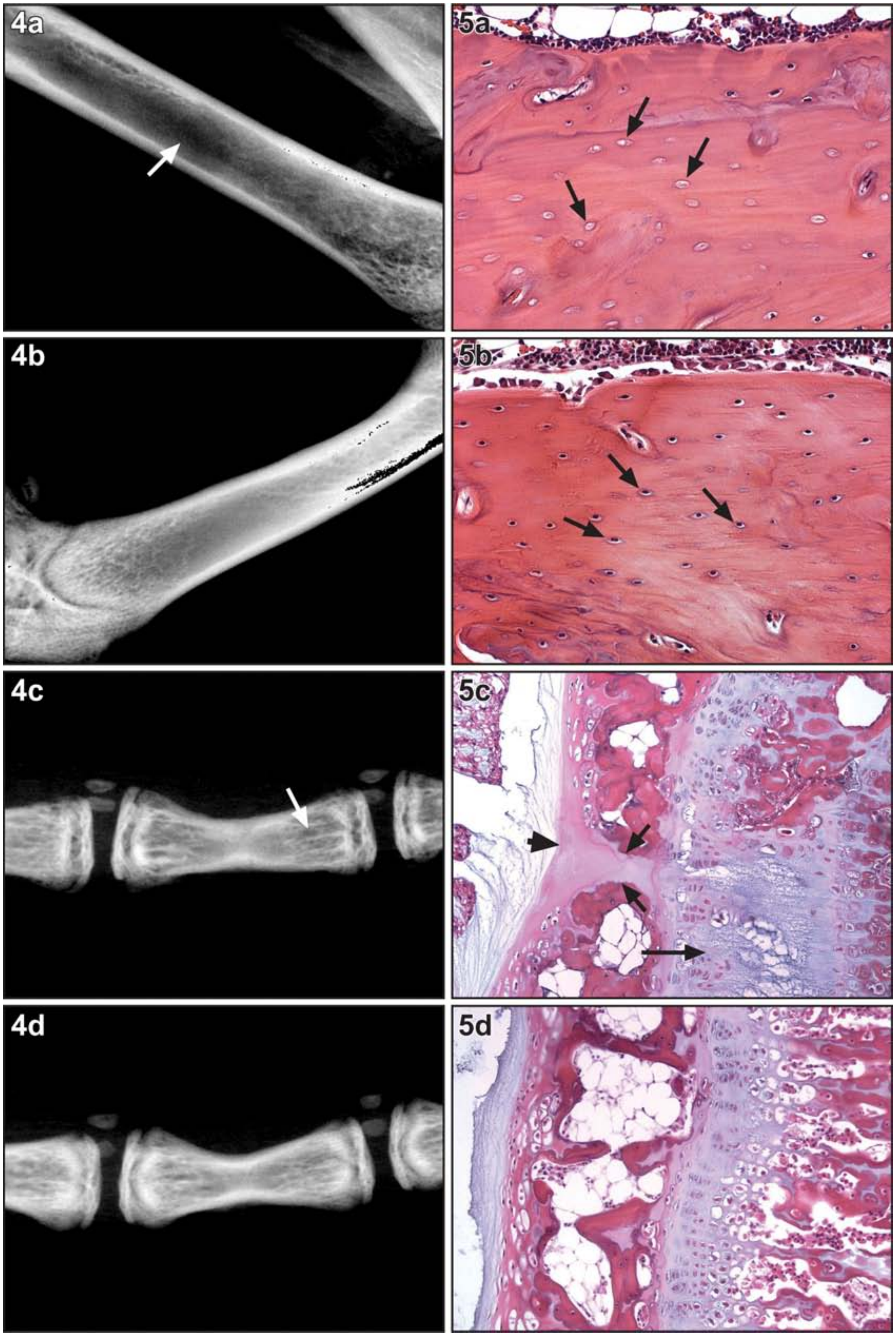

FIGURE 4.—Fischer 344 female rats. (a) Faxitron radiograph of diaphysis in femur 30 days after initiation of treatment with 250 mg/kg/day BE for 4 days. Note decrease in radiographic density in medullary cavity (arrow). (b) Faxitron radiograph of diaphysis in femur of control. (c) Faxitron radiograph of coccygeal vertebra 30 days after initiation of treatment with 250 mg/kg/day BE for 4 days. Note decrease in radiographic density in metaphysis (arrow). (d) Faxitron radiograph of coccygeal vertebra of a control. 5.—Fischer 344 female rats. (a) Osteocytic necrosis (arrows) in femur 30 days after initiation of treatment with 250 mg/kg/day BE for 4 days. H&E. ×20. (b) Normal osteocytes (arrows) in femur of control. H&E. ×20. (c) Necrosis of articular cartilage (arrowhead), epiphyseal bone (short arrows), and growth plate (long arrow) in coccygeal vertebra 30 days after initiation of treatment with 250 mg/kg/day BE for 4 days. H&E. ×20. (d) Normal articular cartilage, epiphyseal bone, and growth plate in coccygeal vertebra of a control. H&E. ×20.

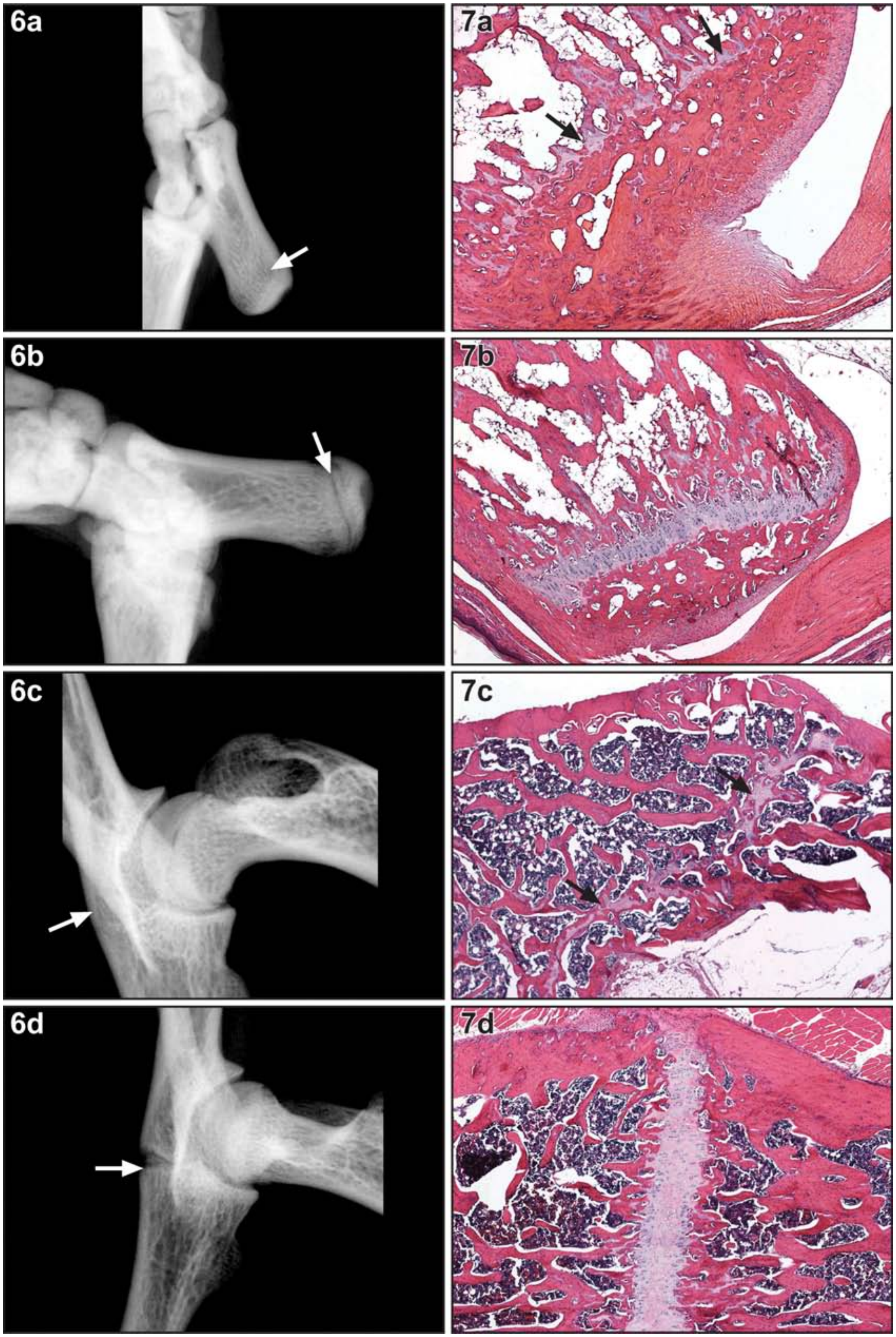

FIGURE 6.—Fischer 344 female rats. (a) Faxitron radiograph of calcaneus 30 days after initiation of treatment with 300 mg/kg/day BE for 4 days. Note premature closure of growth plate (arrow). (b) Faxitron radiograph of calcaneus of control. Note normal growth plate (arrow). (c) Faxitron radiograph of hip joint 30 days after initiation of treatment with 250 mg/kg/day BE for 4 days. Note loss of triradiate cartilage of the acetabulum (arrow). (d) Faxitron radiograph of hip joint of control. Note normal triradiate cartilage of the acetabulum (arrow). 7.—Fischer 344 female rats. (a) Premature closure of growth plate in calcaneus (arrows) 30 days after initiation of treatment with 300 mg/kg/day BE for 4 days. H&E. ×4. (b) Normal growth plate in calcaneus of control. H&E. ×4. (c) Loss of triradiate cartilage of the acetabulum (arrows) 30 days after initiation of treatment with 250 mg/kg/day BE for 4 days. H&E. ×4. (d) Normal triradiate cartilage of the acetabulum of control. H&E. ×4.

administration of this high dose to induce this disseminated thrombotic crisis, the type that is also seen in sickle cell patients. The patterns of thrombosis seen in this study affirm previous studies claiming this to be an appropriate chemically induced animal model for researching human thrombotic disorders (Andrews et al., 1983; Cox and Soni, 1984; Smith, 1996; Nyska et al., 1999b; Eldor and Rachmilewitz, 2002; Ezov et al., 2002; Koshkaryev et al., 2003; Redlich et al., 2004; Shabat et al., 2004).

Erythrocytes in humans with sickle cell anemia may be more prone to aggregation and vascular occlusion, leading to thrombosis (Obeifuna, 1991). Infarctive crisis is the most frequent form of sickle crisis, in which sickled erythrocytes obstruct small blood vessels in many organs, producing severe pain (Bonner and Erslev, 1994). In these patients, the skeleton is a frequent target of thrombosis and infarction, leading to bone and bone marrow infarction, as well as aseptic necrosis of various long bones (Hernigou et al., 1993; Smith, 1996; Hernigou et al., 1998; Kim and Miller, 2002; Hernigou et al., 2003). Disturbances in bone growth due to ischemia of the growth plate have been noted in sickle cell disease (Hernigou et al., 1993, 1998, 2003), other hemoglobinopathies (Johanson, 1990), and cases of local thrombosis induced accidentally in humans (DiFiori and Mandelbaum, 1996; Macnicol and Anagnostopoulos, 2000) or experimentally in animals (Beppu et al., 1989; Tamura et al., 1992; Hou et al., 1993; Shimizu et al., 1995; Kim et al., 2001; Matsuno et al., 2001). In the rats sacrificed 2 hours following the final BE treatment, thrombosis of the periosteal, cortical, and marrow blood vessels was confirmed. Damage to the growth plates of several bones was noted in the radiographs and subsequent histopathological examination of the treated rats sacrificed on day 30.

Interesting findings in the treated animals sacrificed at 30 days that have not been previously demonstrated included a loss of the triradiate cartilage of the acetabulum and a premature closure of the growth plate of the calcaneus. Hip dysplasia is a common complication of sickle cell disease, and the pathogenesis is thought to involve direct damage to the triradiate cartilage (Hernigou et al., 1993). Hip osteonecrosis has become a significant cause of morbidity in sickle cell-disease patients, especially adults, and treatment options are extremely limited for this complication (Mandell and Meek, 1993; Reed and Vichinsky, 1998; Hernigou et al., 2003). Patients with sickle cell disease also may develop a pathognomonic calcaneal lesion related to avascular necrosis of the bone (Rothschild et al., 1997). These findings illustrate even more similarities between this animal model and human thrombotic diseases.

The Faxitron Specimen Radiography System proved to be a useful tool for obtaining high-magnification X-ray images of various bones in the rats sacrificed after 30 days. The Faxitron has, along with a second imaging system, previously been used in mice to quantify the rate of bone healing (Li et al., 2001). It has also been used in imaging human fetuses (Bach-Petersen et al., 1995; Kjaer et al., 1998, 1999; Nolting et al., 1998). Unlike a previous MRI imaging of the bones, the Faxitron was able to distinguish the growth plates and bone diaphyses with high resolution (Shabat et al., 2004). Premature closure of the growth plate was found in many bones of the treated animals, including the coccygeal vertebrae, femur, proximal tibia, lumbar vertebrae, and calcaneus bones. That the Faxitron was also useful in locating areas of medullary necrosis in many of the bones was illustrated by a decreased radiographic density in the medullary cavity. The reason for this decrease was determined histologically to be necrosis in the cortical femur bone of 1 of the treated animals, diagnosed by the presence of empty osteocyte lacunae.

A statistically significant increase occurred in the ratio of the epiphyseal density to the subepiphyseal density in the treated animals, compared to controls, for the lumbar vertebrae and the calcaneus bones. This occurrence was due to decreased radiographic density in the subepiphysis of the treated animals. In the animals examined acutely following BE treatment, thrombosis was found in the end arteries of the subepiphyseal area and in the cortical bone. The infarction of the growth plate due to the thrombosis would lead to deceleration of bone growth and a decrease in the radiographic density of the subepiphyseal area.

That no bone thrombosis was observed in any of the animals examined at 30 days indicated that the ischemic episode was acute. This observation correlates with the findings of previous studies demonstrating that thrombi occurred only in animals sacrificed immediately following the final BE treatment, not in those given a recovery period (Ezov et al., 2002; Redlich et al., 2004; Shabat et al., 2004). The disturbances in growth plates seen only in those animals examined after 30 days correlate with abnormalities of human hemoglobinopathies, in which growth disturbances are frequently not seen until adolescence due to improved hematological management (Johanson, 1990).

That the duration of ischemia is the most important determinant of pediatric growth plate disturbances has been demonstrated previously (Stark et al., 1987; Carey et al., 1990; Tamura et al., 1992; Hou et al., 1993; Shimizu et al., 1995; Sunagawa, 1996). At least 6 hours of ischemia are required before longitudinal growth is affected (Shimizu et al., 1995; Matsuno et al., 2001). The treated animals that were examined by radiography and subsequent histology had endured chronic ischemic injury as a result of the disseminated thrombosis induced by BE. This was illustrated grossly, in the appearance of the tails, as well as histologically. The severe hemolytic anemia induced by BE for at least 4–5 days could also have contributed to a reduction of normal proliferation in the growth plate, due to a decreased oxygen tension (Carey et al., 1990). In the coccygeal vertebrae, thrombosis of large vessels was identified in the animals sacrificed on day 4, and an infarction of the growth plate was seen in the animals sacrificed on day 30, or 26 days after the final treatment. Based on these findings, ischemia due to thrombosis most likely constituted the principal cause of reduced growth plate proliferation in this region. In the other articulations, however, the hemolytic anemia and reduced oxygen tension most likely led to the reduced growth. In future studies using this model, we plan to examine at 4 days those regions that were only examined chronically, such as the calcaneus and triradiate cartilage, to look for thrombosis.

Normal growth plate chondrocytes undergo apoptosis to contribute to longitudinal bone growth (Hatori et al., 1995; Zenmyo et al., 1996). Ischemia and eventual reperfusion, however, lead to an increased rate of chondrocytic cell death by both apoptosis and necrosis (Matsuno et al., 2001).

Ischemia lasting 48 hours causes death to chondrocytes due to interruption of the epiphyseal blood supply (Trutea and Amato, 1960). The severe anemia and thrombosis induced acutely by BE, demonstrated histologically in the rats sacrificed following the final dose, would lead to this ischemic damage.

Those animals sacrificed after 30 days may also have been affected by reperfusion injury. During such injury, oxygen free radicals are produced, causing oxidative stress that may damage proliferating chondrocytes in epiphyseal growth plates, as well as cells in other organs and tissues (McCord, 1985; Weiss et al., 1989; Tamura et al., 1992; Yokoyama et al., 1993; Al-Qattan, 1998). The free radicals directly kill more chondrocytes by destruction of cellular membranes and also increase cellular death signals (Matsuno et al., 2001). The rate of cell death increases with increased ischemia time due to the production of more oxygen free radicals (Yokoyama et al., 1993). These events explain, in part, the pathogenesis of the lesions seen in the growth plates of these animals by both radiographical and histological examination. With such a length of time of ischemia experienced by these rats, however, other pathological alterations, such as residual changes in vascular patency, may also affect growth disturbances (Matsuno et al., 2001).

Normal closure of growth plates in the rat occurs at 11 to 12 months, with the physis of long bones never completely resorbed (Leininger and Riley, 1990; Kilborn et al., 2002). The treated rats that were sacrificed at 30 days and examined by radiography were 15–16 weeks old at the time of sacrifice. Although the control animals were only 10–12 weeks old at the time of sacrifice, the closure seen in the growth plates of several bones by radiography and in the calcaneus and triradiate cartilage by histology is not due to this difference in age between the groups. The treated rats were too young to exhibit such a dramatic loss of epiphyseal cartilage. The measured decrease in width of the growth plate in the femur, tibia, and lumbar vertebra in the treated animal, compared to the control, however, would be more convincing had the rats been of the same age. In future experiments using this animal model, the treatment and control groups must be more carefully age-matched. This matching would also be more helpful in evaluating other measurements, such as the length and width of the bones.

Additional investigations using this model are currently underway, aiming to identify blood biomarkers that reflect the hypercoagulable state occurring in these rats. These biomarkers can then be applied in testing drug efficacy for the acute thrombotic stage of this model.

The lesions seen by the radiographic imaging correlated well with those seen by histological examination. The Faxitron specimen radiography system is a noninvasive tool that can be used in future studies to image the chronic effects of BE exposure on the skeletal system of female F344 rats, an animal model in which treatment modalities can be examined and applied to the chronic effects of a number of human hemolytic diseases associated with thrombotic alterations.

ACKNOWLEDGMENTS

The authors thank JoAnne Johnson, Dr. Gordon Flake, and Dr. Hiroshi Satoh for critically reviewing this manuscript; those at ILS who assisted with this study, especially Dr. Glenda Moser and Theleria Hackett; and members of the histology staff at NIEHS, especially Natasha Clayton, Julie Foley, Tina Jones, Bettie Harris, and Denise Burwell, who provided outstanding technical expertise.

REFERENCES

Aasmoe, L., Winberg, J. O., and Aarbakke, J. (1998). The role of liver alcohol dehydrogenase isoenzymes in the oxidation of glycolethers in male and female rats. *Toxicol Appl Pharmacol* **150**, 86–90.

Al-Qattan, M. M. (1998). Ischemia-reperfusion injury. *J Hand Surg [Br]* **23**, 570–3.

Andrews, C. H., England, M. C. J., and Kemp, W. B. (1983). Sickle cell anemia: an etiological factor in pulpal necrosis. *J Endod* **9**(6), 249–52.

Bach-Petersen, S., Solow, B., Fischer Hansen, B., and Kjaer, I. (1995). Growth in the lateral part of the human skull during the second trimester. *J Craniofac Genet Dev Biol* **15**(4), 205–11.

Beppu, M., Takahashi, F., Tsai, T. M., Ogden, L., and Sharp, J. B. (1989). Experimental replantation of canine forelimbs after 78.5 hours of anoxia. *Plast Reconstr Surg* **84**(4), 642–50.

Bonner, H., and Erslev, A. J. (1994). The blood and the lymphoid organs. In Pathology (E. Rubin and J. L. Farber, eds.), pp. 1022–5. J.B. Lippincott, Philadelphia.

Boorman, G. A., Morgan, K. T., and Uraich, L. C. (1990). Nose, larynx, and trachea. In Pathology of the Fischer Rat (G. A. Boorman, S. L. Eustis, M. R. Elwell, C. A. Montgomery, and W. F. MacKenzie, eds.), pp. 315–37. Academic Press, New York.

Carey, L. A., Weiss, A. P. C., and Weiland, A. J. (1990). Quantifying the effect of ischemia on epiphyseal growth in an extremity replant model. *J Hand Surg [Am]* **15**(4), 625–30.

Chhabra, R. S., Huff, J. E., Schwetz, B. S., and Selkirk, J. (1990). An overview of prechronic and chronic toxicity/carcinogenicity experimental study designs and criteria used by the National Toxicology Program. *Environ Health Perspect* **86**, 313–21.

Cox, G. M., and Soni, N. N. (1984). Pathological effects of sickle cell anemia on the pulp. *J Dent Child* **51**(2), 128–32.

DiFiori, J. P., and Mandelbaum, B. R. (1996). Wrist pain in a young gymnast: unusual radiographic findings and MRI evidence of growth plate injury. *Med Sci Sports Exerc* **28**(12), 1453–8.

Dill, J. A., Lee, K. M., Bates, D. J., Anderson, D. J., Johnson, R. E., Chou, B. J., Burka, L. T., and Roycroft, J. H. (1998). Toxicokinetics of inhaled 2-butoxyethanol and its major metabolite, 2-butoxyacetic acid, in F344 rats and B6C3F1 mice. *Toxicol Appl Pharmacol* **153**(2), 227–42.

Eldor, A., and Rachmilewitz, E. A. (2002). The hypercoagulable state in thalassemia. *Blood* **99**(1), 36–43.

Ezov, N., Levin-Harrus, T., Mittelman, M., Redlich, M., Shabat, S., Ward, S. M., Peddada, S., Nyska, M., Yedgar, S., and Nyska, A. (2002). A chemically induced rat model of hemolysis with disseminated thrombosis. *Cardiovasc Toxicol* **2**(3), 181–94.

Ghanayem, B. I., Sanders, J. M., Clark, A. M., Bailer, J., and Matthews, H. B. (1990). Effects of dose, age, inhibition of metabolism and elimination on the toxicokinetics of 2-butoxyethanol and its metabolites. *J Pharmacol Exp Ther* **253**(1), 136–43.

Ghanayem, B. I., Ward, S. M., Chanas, B., and Nyska, A. (2000). Comparison of the acute hematoxicity of 2-butoxyethanol in male and female rats. *Hum Exp Toxicol* **19**, 185–92.

Halvorsen, A. M., Futrell, N., and Wang, L. C. (1994). Fibrin content of carotid thrombi alters the production of embolic stroke in the rat. *Stroke* **25**(8), 1632–6.

Hatori, M., Klatte, K. J., Teixeria, C. C., and Shapiro, I. M. (1995). End labeling studies of fragmented DNA in the avian growth plate: evidence of apoptosis in terminally differentiated chondrocytes. *J Bone Miner Res* **10**, 1960–8.

Hernigou, P., Allain, J., Bachir, D., and Galacteros, F. (1998). Abnormalities of the adult shoulder due to sickle cell osteonecrosis during childhood. *Rev Rhum [Engl Ed]* **65**(1), 27–32.

Hernigou, P., Bachir, D., and Galacteros, F. (1993). Hip dysplasia, a complication of sickle cell anemia. *Rev Rhum [Ed Fr]* **60**(7–8), 505–13.

Hernigou, P., Bachir, D., and Galacteros, F. (2003). The natural history of symptomatic osteonecrosis in adults with sickle-cell disease. *J Bone Joint Surg Am* **85-A**(3), 500–4.

Hou, S. M., Wang, T. G., and Liu, M. R. (1993). Longitudinal growth after replantation of immature extremities on rats. *J Hand Surg [Am]* **18**(5), 828–32.

Hovav, T., Goldfarb, A., Artmann, G., Yedgar, S., and Barshtein, G. (1999). Enhanced adherence of beta-thalassaemic erythrocytes to endothelial cells. *Br J Haemotol* **106**, 178–81.

Imhof, H., Breitenseher, M., Trattnig, S., Kramer, J., Hofmann, S., Plenk, H., Schneider, W., and Engel, A. (1997). Imaging of avascular necrosis of bone. *Eur Radiol* **7**(2), 180–6.

Institute of Laboratory Animal Resources. (1996). *Guide for the Care and Use of Laboratory Animals*. National Academy Press, Washington, DC.

Johanson, N. A. (1990). Musculoskeletal problems in hemoglobinopathy. *Orthop Clin North Am* **21**(1), 191–8.

Kilborn, S. H., Trudel, G., and Uhthoff, H. (2002). Review of growth plate closure compared with age at sexual maturity and lifespan in laboratory animals. *Contemp Top Lab Anim Sci* **41**(5), 21–6.

Kim, H. K., Su, P. H., and Qui, Y. S. (2001). Histopathologic changes in growth-plate cartilage following ischemic necrosis of the capital femoral epiphysis. An experimental investigation in immature pigs. *J Bone Joint Surg Am* **83-A**(5), 688–97.

Kim, S. K., and Miller, J. H. (2002). Natural history and distribution of bone and bone marrow infarction in sickle hemoglobinopathies. *J Nucl Med* **43**(7), 896–900.

Kjaer, I., Fischer Hansen, B., Reintoft, I., and Keeling, J. W. (1999). Pituitary gland and axial skeletal malformations in human fetuses with spina bifida. *Eur J Pediatr Surg* **9**(6), 354–8.

Kjaer, M. S., Keeling, J. W., Anderson, E., Fischer Hansen, B., and Kjaer, I. (1998). Hand development in trisomy 21. *Am J Med Genet* **79**(5), 337–42.

Koshkaryev, A., Barshtein, G., Nyska, A., Ezov, N., Levin-Harrus, T., Shabat, S., Nyska, M., Redlich, M., Tsipis, F., and Yedgar, S. (2003). 2-Butoxyethanol enhances the adherence of red blood cells. *Arch Toxicol* **77**(8), 465–9.

Leininger, J. R., and Riley, M. G. I. (1990). Bones, joints and synovia. In Pathology of the Fischer Rat (G. A. Boorman, S. L. Eustis, M. R. Elwell, C. A. Montgomery, W. F. MacKenzie eds.), pp. 209-14. Academic Press, Inc., San Diego, CA.

Li, X., Gu, W., Masinde, G., Hamilton-Ulland, M., Rundle, C. H., Mohan, S., and Baylink, D. J. (2001). Genetic variation in bone-regenerative capacity among inbred strains of mice. *Bone* **29**(2), 134–40.

Long, P. H., Maronpot, R. R., Ghanayem, B. I., Roycroft, J. H., and Nyska, A. (2000). Dental pulp infarction in female rats following inhalation exposure to 2-butoxyethanol. *Toxicol Pathol* **28**, 246–52.

Macnicol, M. F., and Anagnostopoulos, J. (2000). Arrest of the growth plate after arterial cannulation in infancy. *J Bone Joint Surg Br* **82**(2), 172–5.

Mandell, G. A., and Meek, R. S. (1993). Infarctions of the ilia in young patients with sickle hemoglobinopathies. *Clin Nucl Med* **18**(7), 558–60.

Matsuno, T., Ishida, O., Arihiro, K., Sunagawa, T., Mori, N., and Ikuta, Y. (2001). Cell proliferation and death of growth plate chondrocyte caused by ischemia and reperfusion. *Microsurgery* **21**(1), 30–6.

McCord, J. M. (1985). Oxygen-derived free radicals in postischemic tissue injury. *N Engl J Med* **312**, 159–63.

Momotani, E., Yabuki, Y., Miho, H., Ishikawa, Y., and Yoshino, T. (1985). Histopathological evaluation of disseminated intravascular coagulation in Haemophilus somnus infection in cattle. *J Comp Pathol* **95**, 15–23.

Nolting, D., Hansen, B. F., Keeling, J., and Kjaer, I. (1998). Prenatal development of the normal human vertebral corpora in different segments of the spine. *Spine* **23**(21), 2265–71.

Norman, D., Reis, D., Zimman, C., Misselvich, I., and Boss, J. H. (1998). Vascular deprivation-induced necrosis of the femoral head of the rat. An experimental model of avascular osteonecrosis in the skeletally immature individual or Legg-Perthes disease. *Int J Exp Pathol* **79**, 173–81.

Nyska, A., Maronpot, R., and Ghanayem, B. I. (1999a). Ocular thrombosis and retinal degeneration induced in female F344 rats by 2-butoxyethanol. *Hum Exp Toxicol* **18**, 577–82.

Nyska, A., Maronpot, R., Long, P., Roycroft, J., Hailey, J., Travlos, G., and Ghanayem, B. (1999b). Disseminated thrombosis and bone infarction in female rats following inhalation exposure to 2-butoxyethanol. *Toxicol Pathol* **27**(3), 287–94.

Nyska, A., Moomaw, C. R., Ezov, N., Shabat, S., Levin-Harrus, T., Nyska, M., Redlich, M., Mittelman, M., Yedgar, S., and Foley, J. F. (2003). Ocular expression of vascular cell adhesion molecule (VCAM-1) in 2-butoxyethanol-induced hemolysis and thrombosis in female rats. *Exp Toxicol Pathol* **55**(4), 231–6.

Obeifuna, P. C. (1991). Rouleaux formation in sickle cell traits. *J Trop Med Hyg* **94**, 42–4.

Redlich, M., Maly, A., Aframian, D., Shabat, S., Ezov, N., Levin-Harrus, T., Nyska, M., and Nyska, A. (2004). Histopathologic changes in dental and oral soft tissues in 2-butoxyethanol-induced hemolysis and thrombosis in rats. *J Oral Pathol Med* **33**, 1–6.

Reed, W., and Vichinsky, E. P. (1998). New considerations in the treatment of sickle cell disease. *Annu Rev Med* **49**, 461–74.

Rothschild, B. M., Sebes, J. I., and Hershkovitz, I. (1997). Microfoci of avascular necrosis in sickle cell anemia: pathophysiology of the dot dash pattern. *Clin Exp Rheumatol* **15**(6), 663–6.

Shabat, S., Nyska, A., Long, P. H., Goelman, G., Abramovitch, R., Ezov, N., Levin-Harrus, T., Peddada, S., Redlich, M., Yedgar, S., and Nyska, M. (2004). Osteonecrosis in a chemically induced rat model of human hemolytic disorders associated with thrombosis—a new model for avascular necrosis of bone. *Calcif Tissue Int* **74**(3), 220–8.

Shimizu, H., Tsai, T. M., and Firrell, J. C. (1995). Effect of ischemia and three different perfusion solutions on the rabbit epiphyseal growth plate. *Microsurgery* **16**(9), 639–45.

Smith, J. A. (1996). Bone disorders in sickle cell disease. *Hematol Oncol Clin North Am* **10**(6), 1345–55.

Stark, R. H., Matloub, H. S., Sanger, J. R., Cohen, E. B., and Lynch, K. (1987). Warm ischemic damage to the epiphyseal growth plate: a rabbit model. *J Hand Surg [Am]* **12**, 54–61.

Sunagawa, T. (1996). Longitudinal bone growth after replantation in immature rats. *J Hiroshima Univ School Med* **44**, 43–53.

Tamura, Y., Inoue, G., Miura, T., Ishiguro, N., and Shimizu, T. (1992). Reperfusion injury in bone: effects of CV-3611, a free radical scavenger, on ischemic revascularized bone grafts in rats. *J Reconstr Microsurg* **8**(6), 471–9.

Trutea, J., and Amato, V. P. (1960). The vascular contribution to osteogenesis. 3. Changes in the growth cartilage caused by experimentally induced ischemia. *J Bone Joint Surg Br* **42**, 571–87.

Udden, M. M. (2002). In vitro sub-hemolytic effects of butoxyacetic acid on human and rat erythrocytes. *Toxicol Sci* **69**, 258–64.

Weiss, A. C., Carey, L. A., Randolph, M. A., Moore, J. R., and Weiland, A. J. (1989). Oxygen free radical scavengers improve vascular patency and bone-muscle cell survival in an ischemic extremity replant model. *Plast Reconstr Surg* **84**, 117–23.

Yedgar, S., Hovav, T., and Barshtein, G. (1999). Red blood cell intercellular interactions in oxidative stress states. *Clin Hemorheol Microcirc* **21**, 189–93.

Yokoyama, K., Itoman, M., Takagishi, K., Sekiguchi, M., Yamamoto, M., and Nakamura, K. (1993). The effect of superoxide production on the replantation of rat limbs after cold ischemia. *J Reconstr Microsurg* **9**, 61–8.

Zenmyo, M., Komiya, S., Kawabata, R., Sasaguri, Y., Inoue, A., and Morimatsu, M. (1996). Morphological and biochemical evidence for apoptosis in the terminal hypertrophic chondrocytes of the growth plate. *J Pathol* **180**, 430–3.

Zhao, W., Byrne, M. H., Wang, Y., and Krane, S. M. (2000). Osteocyte and osteoblast apoptosis and excessive bone deposition accompany failure of collagenase cleavage of collagen. *J Clin Invest* **106**(8), 941–9.